Nature Environment and Pollution Technology
An International Quarterly Scientific Journal

p-ISSN: 0972-6268
(Print copies up to 2016)
e-ISSN: 2395-3454

Vol. 25 | No. 3 | Article ID B4392 | 2026

Original Research Paper

https://doi.org/10.46488/NEPT.2026.v25i03.B4392

Open Access Journal

Eco-Friendly Neem-Based Corrosion Inhibitor Coatings for Reinforced Concrete: Performance, Sustainability and Cost Assessment

Satya Prakash and Nishant Kumar†
Department of Civil Engineering, Sharda University, Greater Noida, India
†Corresponding author: Nishant Kumar; Nishant.kumar4@sharda.ac.in

Abbreviation: Nat. Env. & Poll. Technol.
Website: www.neptjournal.com

Received: 11-09-2025
Revised: 17-11-2025
Accepted: 27-11-2025

Key Words:

Corrosion inhibitors
Organic inhibitors
Sustainable construction
Environmentally safe
Eco-friendly coatings
LCA assessment

Citation for the Paper:

Prakash, S. and Kumar, N., 2026. Eco-friendly neem-based corrosion inhibitor coatings for reinforced concrete: Performance, sustainability, and cost assessment. *Nature Environment and Pollution Technology*, 25(3), B4392. https://doi.org/10.46488/NEPT.2026.v25i03. B4392

Note: From 2025, the journal has adopted the use of Article IDs in citations instead of traditional consecutive page numbers. Each article is now given individual page ranges starting from page 1.

ABSTRACT

Corrosion of reinforcement in concrete is a critical durability challenge that undermines the service life and increases the maintenance costs of infrastructure. Although conventional inorganic inhibitors, such as zinc, are effective, they are associated with high costs and environmental concerns, necessitating the development of sustainable alternatives. This study investigated the potential of Azadirachta indica (Neem) powder as a green, bio-based corrosion inhibitor coating for reinforcing steel, with its performance benchmarked against zinc coatings. Reinforced M30 grade concrete specimens were subjected to chloride-induced accelerated corrosion for 365 days and evaluated through half-cell potential, weight and diameter loss, pullout bond strength, and surface morphology using SEM. Neem-coated specimens demonstrated a 47.5% reduction in half-cell potential and a 54% improvement in bond strength relative to uncoated specimens, closely matching zinc-coated samples, whose performance differences were not statistically significant. Life cycle assessment revealed that Neem coatings reduced the carbon footprint by up to 43%, whereas cost analysis showed a 39.6% reduction in per-meter coating cost compared to zinc. The findings highlight neem-based coatings as a sustainable, cost-effective, and eco-friendly solution offering performance comparable to zinc, thereby supporting resilient and environmentally responsible construction practices.

1. INTRODUCTION

Concrete and steel structures deteriorate over time owing to poor construction practices, inadequate maintenance, and exposure to aggressive environments, such as carbonation and chlorides, which accelerate reinforcement corrosion and reduce their service life. Effective durability planning and preventive measures require an understanding of the corrosion mechanisms (Ghanaati et al. 2022). Corrosion, driven by chemical and electrochemical processes, leads to cracking, spalling, and staining of concrete surfaces, exposing the reinforcement to further degradation and progressive loss of structural integrity (Singh et al. 2022, Zhao et al. 2019). Chloride and sulfate ions originating from de-icing salts, marine exposure, and industrial pollutants are major initiators of corrosion (Abirami & Sangeetha 2022). Their ingress is exacerbated by inadequate cover, poor compaction, microcracks, and environmental factors such as temperature variations, humidity changes, and freeze–thaw cycles, with geographical and industrial conditions further intensifying deterioration (Bajaj & Khurpade 2024). To counter these effects, corrosion inhibitor coatings are increasingly used to provide a protective barrier that restricts chloride and sulfate penetration and suppresses electrochemical reactions at the steel surface (Kamarska 2024, Jiang et al. 2025a, Kumar et al. 2025). Organic inhibitors form adsorbed protective films, whereas inorganic inhibitors contribute to passivation through chemical interactions with the cementitious matrix (Goni & Mazumder 2019, Söylev & Richardson 2008). Both systems have shown improved durability and mechanical performance under aggressive exposure (Hao et al. 2023, Kumar & Saharan 2022, Sharma et al. 2022, Sharmila & Vasanthi 2024).

Chloride-induced corrosion is particularly severe because chloride ions penetrate the concrete cover and destroy the passive oxide layer that normally protects steel in an alkaline pore environment (Ega et al. 2024). Once depassivated, steel undergoes localized anodic dissolution, forming ferrous ions that react with chloride to produce soluble complexes, which subsequently hydrolyze to form ferrous hydroxide and hydrochloric acid (Jiang et al. 2025b, Ovari et al. 2025). This acid regenerates chloride ions, thereby creating a self-sustaining corrosion cycle (Shehnazdeep & Pradhan 2022). The resulting rust products occupy a much larger volume, generating tensile stresses that cause cracking, delamination, and spalling of the concrete cover (Liu & Shi 2024). Fig. 1 illustrates the process of chloride-induced corrosion in concrete.

Fig. 2 illustrates the stages of deterioration caused by reinforcement corrosion in concrete and its effects on structural performance. In the initial phase, the steel reinforcement is protected by a passive oxide film formed in the alkaline pore solution. When chloride ions penetrate or carbonation lowers the alkalinity, this passive layer breaks down, initiating active corrosion. The anodic dissolution of steel generates expansive rust products that occupy several times the volume of the original metal (McCafferty 2010). This expansion produces hoop stresses at the steel–concrete interface, thereby creating pressure on the cover concrete. When the stress exceeds the tensile strength of the concrete, microcracks form, which later develop into visible cracks. These pathways allow more chloride, oxygen, and moisture to enter, creating a self-sustaining cycle of deterioration (Umamathi et al. 2024).

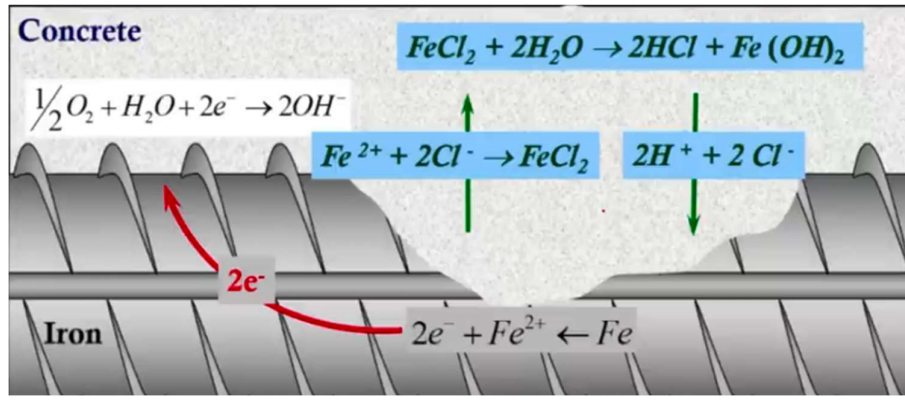

Fig. 1: Chloride-induced corrosion in concrete (Al-Amiery et al. 2024).

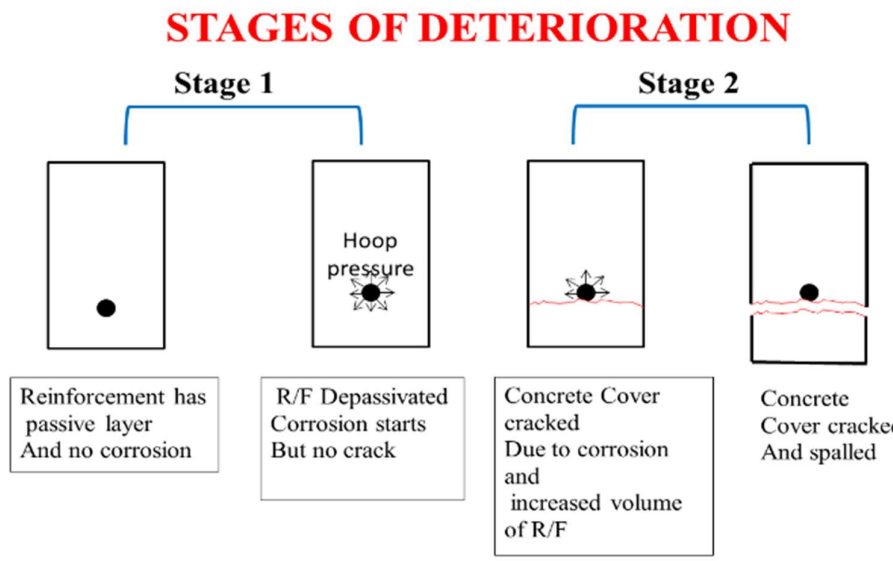

Fig. 2: Stages of deterioration in concrete due to corrosion.

In advanced stages, the concrete cover spalls, exposing the reinforcement to the environment and reducing both its cross-sectional area and structural capacity.

To mitigate such degradation, corrosion inhibitor coatings have been used; however, their effectiveness must be validated using electrochemical evaluation and pull-out tests. Half-cell potential measurements are widely used to indicate corrosion probability, although they do not provide actual rates. Thus, it is complemented by direct methods, such as weight loss and diameter reduction, which measure physical damage. Bond strength evaluation is equally important because corrosion-induced cracking and rust expansion reduce steel–concrete adhesion, directly affecting structural safety. Therefore, pull-out bond tests provide critical data on the mechanical effects of corrosion. By combining the half-cell potential, weight loss, diameter loss, and bond strength assessments, a comprehensive evaluation of the inhibitor performance can be achieved. Such testing ensures that organic coatings, including neem-based systems, are validated not only for corrosion resistance but also for maintaining durability and bonds in reinforced concrete structures.

Fig. 3 presents a comprehensive classification of strategies for corrosion protection, outlining the principal approaches adopted to mitigate the degradation of materials in aggressive environments. At the highest level, corrosion protection can be achieved through four broad measures: coatings, environmental modification, material selection, and the use of corrosion inhibitors. Coatings serve as physical barriers between the substrate and corrosive medium and may be organic (such as paints and polymers), inorganic (such as metallic or ceramic films), or hybrid systems combining both categories. Environmental modification strategies target the external conditions that drive corrosion, including temperature, pressure, pH, salt concentration, and humidity (Casanova et al. 2023). This category also encompasses electrochemical methods, such as anodic protection, which stabilizes a passive film on the metal surface by applying controlled potentials, and cathodic protection, which can be implemented via sacrificial anodes, galvanization, or impressed current systems.

Another critical strategy involves the judicious selection of materials that inherently resist corrosion. This includes the use of metallic materials such as corrosion-resistant alloys and stainless steels, as well as non-metallic alternatives such as ceramics, plastics, graphite, and rubbers, which offer superior performance in highly corrosive or specialized applications (Tarabin et al. 2023). The final category

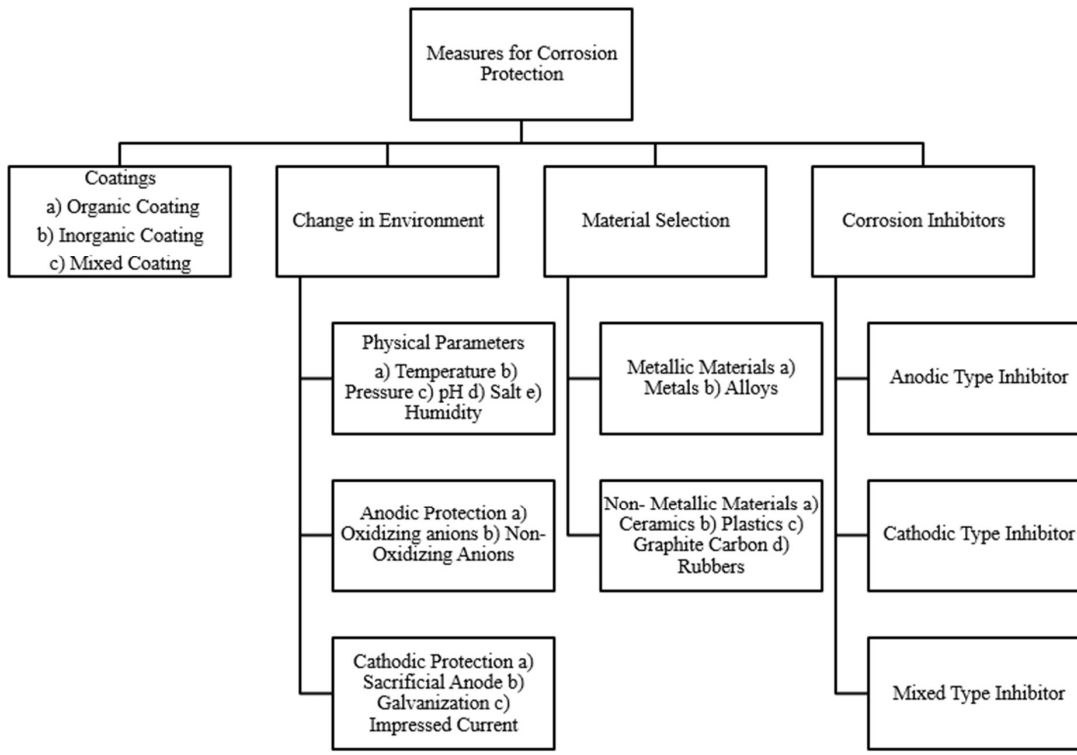

Fig. 3: Measures for corrosion protection (Bajaj & Khurpade 2024, Bolzoni et al. 2022, Casanova et al. 2023, Chen et al. 2023, Li et al. 2023, Nóvoa & Pérez 2023).

focuses on corrosion inhibitors, which are chemical compounds introduced into the environment to suppress electrochemical reactions on metal surfaces. These can function as anodic inhibitors, promoting the formation of protective oxide layers; cathodic inhibitors, reducing the rate of cathodic reactions such as oxygen reduction; or mixed-type inhibitors, providing simultaneous protection at both anodic and cathodic sites (Verma et al. 2024). This study aims to experimentally evaluate neem-based organic coatings for reinforcing steel under chloride-induced corrosion conditions, comparing their performance with that of zinc coatings in terms of electrochemical behavior, bond strength, surface morphology, and sustainability metrics. A detailed literature review of the findings of various corrosion inhibitors used in concrete and the research gap is provided in Table 1.

2. RESEARCH GAP AND RESEARCH SIGNIFICANCE

Research on corrosion inhibitors in concrete has explored admixtures, epoxy coatings, and surface treatments; however, significant challenges remain. Many existing methods suffer from high costs, dosage sensitivity, potential adverse effects on mechanical properties, and limited long-term durability. Admixture-based inhibitors are irreversible once added to fresh concrete, and improper dosage can reduce the strength or even accelerate corrosion. Their performance also declined in cracked concrete. Additionally, several conventional inhibitors, such as chromates and phosphates, pose environmental and health concerns, whereas compatibility issues and limited field-scale data further restrict their reliability. These limitations highlight

Table 1: Comprehensive analysis of the use of corrosion inhibitors in concrete.

Reference	Methods (Material/Exposure/ Measurement)	Findings	Research Gap
(Liu et al. 2025)	Admixture at 0.5–1.5% microstructure (porosity), electrochemistry, and depassivation delay.	Porosity decreased by up to ~69%, delaying steel depassivation and improving electrochemical indices.	Data under mechanical loading and cracked concrete, compatibility with SCMs, and field-scale validation.
(Krishnanjana & Ganesh 2025)	Admixture (3.5–17.5 g), weight loss and electrochemical tests and short-term exposure.	~83% efficiency at 7 g for 7-day exposure.	Short duration, chloride ingress/bond strength effects not assessed, and scale-up dosage guidance missing.
(Suhas et al. 2025)	Admixture, electrochemistry + surface analysis + quantum chemistry & MD simulations.	Chitosan achieved up to ~92.6% efficiency, with mechanistic support from modeling.	The translation of molecular findings to RC elements, their influence on fresh/ concrete properties, and long-term bonds has not been reported.
(Suhas et al. 2025)	Discusses the performance of inhibitors in cracked RC.	Some inhibitors may be ineffective or even accelerate corrosion in the cracks.	Protocols that address crack widths, delivery to exposed steel, and monitoring strategies are required.
(Cao et al. 2025)	Surface-applied (migrating) and computational/mechanistic views.	Potential for in-situ protection of existing RC via migration.	Coupled effects with real chloride profiles, quantifying penetration/ retention and bond effects.
(Liu et al. 2024)	Admixture, optimal ~2 $g.L^{-1}$, chloride-induced corrosion, half-cell + steel weight loss.	Approximately 40% improvement in inhibition efficiency was observed at the optimal dose.	Durability beyond laboratory exposure, synergy with nitrites/SCMs, and structural-scale demonstration.
(Okeniyi et al. 2018)	Plant extract used as an admixture (~0.0833% of cement) with sodium nitrite, RC specimens in 3.5% NaCl, LPR/half-cell/electrochemical tests.	Very high inhibition efficiency (~99.35%) in chloride medium, the strength was not adversely affected.	Long-term durability and field validation, optimum dosage window, and interaction with other admixtures have not been established.
(Okeniyi et al. 2016)	Admixture in concrete beams, 3.5% NaCl immersion, Linear Polarization Resistance, and compressive strength check.	The TEA inhibitor was outperformed, with ~93.6% inhibition and ~5.4% compressive strength improvement.	The mechanism at the steel–concrete interface and bond behavior were not quantified, and the performance under cracking was not studied.
(Montes-García et al. 2015)	Admixture in HPC, variable w/c and 20% FA, wet–dry cycles (2/day) for 1 year, and electrochemical monitoring.	12.5 $L.m^{-3}$ $Ca(NO_2)_2$ with 20% FA effectively reduced the corrosion rates in the low w/c ratio mixes.	Performance envelope for different concretes, effects on setting/air-voids, life-cycle cost vs. performance, and unresolved issues.
(De Schutter & Luo 2004)	Review of admixture inhibitors' effects on fresh/hardened properties.	Risks of set alteration, air-void changes, strength loss, and irreversibility once cast.	Application guidelines for safe windows and compatibility testing with modern admixtures are required.

the need for sustainable and localized protection strategies. Surface-applied coatings offer a promising alternative by targeting the steel–concrete interface, where corrosion initiates, without altering the bulk concrete properties. Despite this advantage, coating-based applications of plant-derived organic inhibitors remain underexplored, particularly their ability to provide corrosion resistance while maintaining steel–concrete bond strength. This study addresses this gap by evaluating Azadirachta indica (Neem powder) as a reinforcement coating for steel bars exposed to chloride corrosion. The investigation assessed the electrochemical behavior through half-cell potential measurements, supported by weight loss, diameter loss, and bond strength tests, and benchmarks Neem's performance against zinc-coated and uncoated specimens to evaluate its durability and sustainability benefits.

3. MATERIALS AND METHODS

This section describes the experimental procedure and methods of analysis adopted to validate the efficacy of Azadirachta indica (Neem Powder) as a green corrosion inhibitor for steel rebars in chloride-induced corrosion environments, along with Zinc Powder inorganic inhibitor coatings. The Neem (Azadirachta indica) powder used in this study was procured from a commercial supplier (IndiaMART, Uttar Pradesh, India). According to the supplier's laboratory certificate, the powder contains approximately 18–22% azadirachtin, 5–7% nimbin, and 3–5% saponins, which are the active components that contribute to corrosion inhibition in steel. The moisture content was below 8%, and the particle size was in the range of 75–150 µm. This study combined measurements of potential difference, that is, half-cell potentiometer readings, weight loss, diameter loss, and bond strength. The experimental methods and materials are presented in detail below. The experimental procedure was designed to systematically investigate the corrosion inhibition performance of an organic coating for steel reinforcement bars in comparison with that of an inorganic coating. This study involved preparing and testing three distinct categories of steel bars: control specimens (uncoated), single-coat organic inhibitor-coated specimens, and single-coat inorganic inhibitor-coated specimens under simulated chloride-induced corrosion conditions. The reinforcement bars were initially cleaned with sandpaper, and a coating paste of inhibitor and linseed oil was prepared in a 1:1.5 ratio by weight, which yielded a viscous paste. The inhibitor paste was applied manually using a bristle brush, and the coating thickness was verified at three locations along the bar using a digital micrometer (±0.02 mm accuracy) to ensure a uniform coating. The resulting coating thickness ranged between 1.0–1.3 mm, with a measured standard deviation of ±0.12 mm across all coated samples with a total coating paste of 35 – 40 $g.mL^{-1}$. The bars were then sun-dried for 24 h and used for casting concrete specimens. For each coating regime, ten cylindrical specimens (a total of 30 samples) were cast using M30 grade concrete with a single reinforcement bar of 16 mm diameter embedded centrally with a cover of 10 mm from the bottom and a total embedded length of 290 mm. After standard moist curing for 28 d, the samples were exposed to chloride-induced corrosive conditions for an extended period of 365 d to simulate a corrosive environment. To accelerate and standardize the corrosion process, all the specimens were subjected to an accelerated corrosion setup. Once the samples were subjected to accelerated corrosion, periodic half-cell potentiometer measurements were conducted to study the effectiveness of the corrosion inhibitor coatings in controlling the corrosion rate. Furthermore, after 365 days, the bond strength of the cast samples was evaluated using a standard pull-out test in accordance with IS 2770: Part 1(1967). After 365 days, the samples were broken, and the reinforcement bars were extracted to measure weight loss and diameter loss. The surface analysis of the coated and neem-coated bars was performed using Scanning Electron Microscopy (SEM). SEM analysis was performed using a ZEISS EVO Scanning Electron Microscope operated in SE1 mode. Micrographs were captured at a magnification of 1.00 kX, an accelerating voltage (EHT) of 15.00 kV, and a working distance (WD) of 8.5 mm. Images were recorded at a scale of 20 µm to observe the corrosion product morphology and coating characteristics. The mix design of the M30 grade of concrete was performed using the IS10262:2019 guidelines, and the details are provided in Table 2.

To simulate the corrosive environment, the cast samples were subjected to the impressed current method. To further accelerate the corrosive environment, the samples were immersed in 3.5% NaCl (Sodium Chloride) solution. A reference reinforcement rod was immersed in the solution, which was used as a cathode, that is, the negative terminal, and the exposed end of the reinforcement bar in the cast samples was used as an anode, that is, the positive terminal, as shown in Fig. 4. The samples were exposed to an accelerated

Table 2: Mix proportions of M30 grade concrete.

Parameter	Quantity	Units
Cement	319.13	kg
Fine aggregate	625	kg
Coarse aggregate	1254	kg
Water	158	kg
Superplasticizer	2.42	kg
Mix Ratio	1:1.96:3.93	

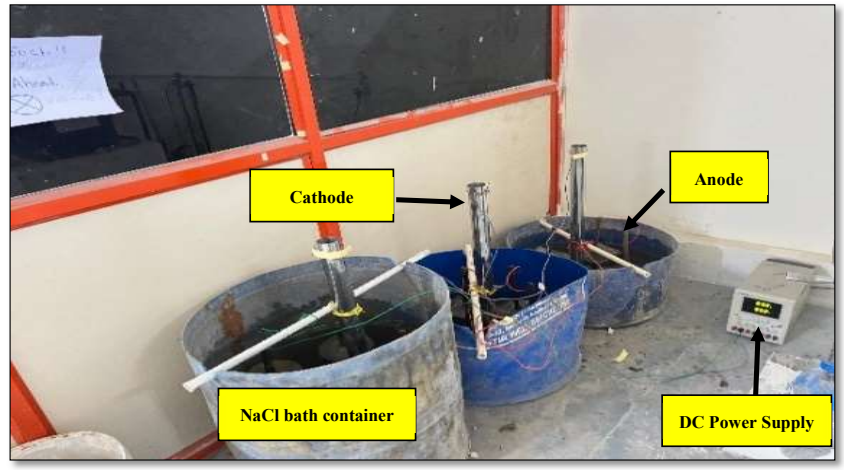

Fig. 4: Accelerated corrosion setup.

corrosion setup, and the corrosion levels were checked and recorded weekly using a half-cell potentiometer. Each half-cell potential measurement was recorded using a calibrated digital potentiometer with a measurement uncertainty of ±5 mV. For accuracy, the reported values represent the average of three consecutive readings taken at 30-second intervals. The samples subjected to the accelerated corrosion setup provided insights into the performance of the corrosion inhibitor coatings in a corrosive environment. The average potential values in (-mV) were obtained from the Half-Cell Potentiometer Test as per ASTM C-876 -15 standards. The Voltage limit was set between 3 and 5 V, and the current was 35.2mA for moderate acceleration for 365 days.

Assessing bond strength is critical for understanding the interaction between concrete and reinforcing steel, which directly influences the structural performance of reinforced concrete elements. The bond strength of concrete primarily depends on the grade of concrete and the type of reinforcement bar used. Furthermore, corrosion can significantly affect the bond strength of concrete, resulting in debonding failure and progressive collapse of the structure. In this study, bond strength was evaluated using the pull-out test method in accordance with IS 2770 (Part 1): 1960. Failure occurs in the form of slippage of the bar from the concrete, indicating bond failure. The various failure patterns, that is, cracks developed on the concrete surface, also indicate the type of bonding between the steel and concrete. A microcrack indicates a good bond of the reinforcement bar, with the minimum value of the slippage, and a major crack indicates poor bond behavior of steel and concrete, with the maximum value of the slippage. The initial weights of the samples prior to casting were recorded, and the final weights of the reinforcement bars were recorded after the pullout test. The corroded steel bars were then carefully cleaned using sandpaper to remove the corrosion products, surface deposits, and any remaining concrete residue. Similarly, the final diameter of the reinforcement bar was recorded after cleaning to evaluate the diameter loss.

4. RESULTS AND DISCUSSION

4.1. Comparative Analysis of Organic and Inorganic Inhibitor Coatings in Corrosion Mitigation

The corrosion assessment results obtained after 365 days of exposure in the accelerated corrosion setup clearly demonstrate significant differences in the performance of the uncoated, neem-coated, and zinc-coated specimens, as discussed in Table 3.

Table 3: Corrosion assessment of organic and inorganic corrosion inhibitors.

Description	Sample		
	Uncoated	Neem Coated	Zinc Coated
Average Half Cell Potentiometer Values [-mV]	273.98	143.79	150.69
Maximum Half Cell Potentiometer Values [-mV]	413.32	217.52	227.03
Average Final Weight [g]	457.10	494.79	494.32
Average Weight Loss [g]	0.927	0.692	0.689
Average Diameter Loss [mm]	0.720	0.678	0.677

Half-cell potential measurements indicated that the uncoated sample had the highest average potential of –273.98 mV, with a maximum of –413.32 mV, which was well below the corrosion threshold, suggesting significant corrosion activity. In contrast, neem-coated and zinc-coated samples showed much lower average potentials of –143.79 mV and –150.69 mV, with maximum values of –217.52 mV and –227.03 mV, respectively, reflecting a substantial reduction in corrosion. Weight measurements supported these findings. The uncoated samples recorded an average final weight of 457.10 g, corresponding to a weight loss of 0.927 g. Neem-coated and zinc-coated samples retained higher weights of 494.79 g and 494.32 g, respectively, with lower weight losses of 0.692 g and 0.689 g. Diameter measurements similarly showed that uncoated samples lost 0.720 mm on average, while neem- and zinc-coated specimens lost only 0.678 and 0.677 mm, respectively. These observations indicate that both coatings effectively limited material degradation, with nearly identical performance in terms of weight retention and dimensional stability. The percentage reduction compared to that of the uncoated samples further highlights the protective efficiency. Neem coatings reduced the average and maximum half-cell potentials by 47.52% and 47.37%, respectively, whereas zinc coatings achieved reductions of 45.00% and 45.07%, respectively. These values fall within the measurement uncertainty of the half-cell potentiometer (±5 mV); therefore, Neem and Zn coatings can be considered statistically equivalent in suppressing electrochemical activity, and the differences should not be interpreted as performance superiority. The inhibitory action of the neem coating can be attributed to the adsorption of its phytochemical constituents, particularly terpenoids, flavonoids, azadirachtin, and nimbin, onto the steel surface. These molecules contain polar functional groups (–OH, –C=O, –C–O–C–, and aromatic rings) capable of donating lone-pair electrons to the vacant d-orbitals of iron atoms, forming a coordinated protective layer. This adsorbed film reduces the active anodic and cathodic reaction sites, thereby restricting chloride interactions and suppressing the corrosion process. The presence of long-chain organic compounds also enhances hydrophobicity, contributing to a more stable barrier. Weight retention improved by 8.25% for neem and 8.14% for zinc, with weight loss decreasing by 25.35% and 25.67%, respectively. Diameter reduction was also limited, showing 5.83% for neem oil and 5.97% for zinc. All corrosion measurements represent the mean of ten specimens, and the corresponding standard deviation values are included to indicate data variability. A one-way ANOVA was performed to compare the corrosion performance across the groups. The differences between the Neem- and Zinc-coated specimens were statistically insignificant ($p > 0.05$), indicating comparable protective behavior.

Overall, these results confirm that neem coatings perform comparably to zinc in mitigating corrosion, preserving structural mass, and limiting dimensional loss. The data demonstrate that neem-based coatings can serve as a sustainable, bio-derived alternative to conventional zinc coatings, offering equivalent protective efficiency and potentially providing environmental benefits.

4.2. Bond Strength Assessment of Coated and Uncoated Bars

To evaluate the effectiveness of the coatings in retaining bond strength, standard pull-out tests were performed in accordance with IS 2770: Part 1 (1967). These tests were performed on neem-coated samples and compared with zinc-coated (inorganic inhibitor) and uncoated specimens. The slip in the reinforcement bars and the ultimate load were recorded using a pull-out testing apparatus, and the bond strength was subsequently calculated.

The bond strength assessment of the coated and uncoated specimens highlights a clear enhancement in interfacial performance due to the application of neem and zinc coatings (Table 4).

Table 4: Comparative assessment pull-out test of organic and inorganic corrosion inhibitors.

Parameter	Uncoated	Neem Coated	Zinc Coated
Maximum Slippage [mm]	6.11	3.79	3.28
Maximum Ultimate Load [kN]	28.04	40.2	44.23
Maximum Bond Strength [MPa]	1.92	2.76	3.03
Minimum Slippage [mm]	5.25	3.45	2.86
Minimum Ultimate Load [kN]	22.39	37.82	41.8
Minimum Bond Strength [MPa]	1.54	2.59	2.87
Average Slippage [mm]	5.69	3.67	3.12
Average Ultimate Load [kN]	25.11	38.75	42.96
Average Bond Strength [MPa]	1.72	2.66	2.95

The uncoated samples exhibited relatively poor bonding behavior, with an average slip-page of 5.69 mm, an average ultimate load of 25.11 kN, and an average bond strength of 1.72 MPa. In contrast, the neem-coated specimens

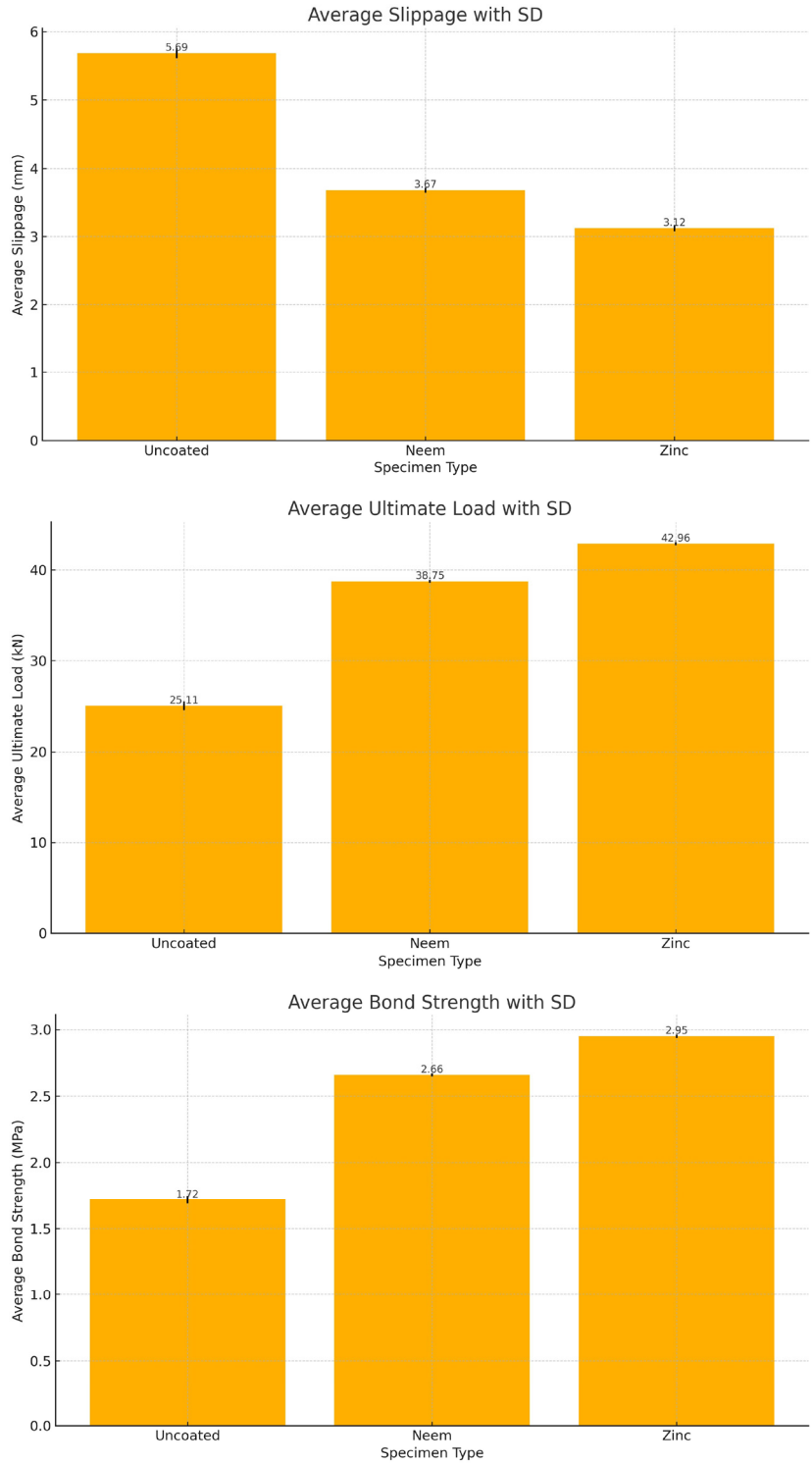

Fig. 5: Standard deviations along with the error bars of the measured corrosion parameters.

demonstrated significantly improved results, with an average slip-page reduced to 3.67 mm, an average ultimate load increased to 38.75 kN, and an average bond strength increased to 2.66 MPa. Similarly, the zinc-coated specimens exhibited the highest performance, with an average slip-page of only 3.12 mm, an ultimate load of 42.96 kN, and an average bond strength of 2.95 MPa, underscoring the superior reinforcement-matrix interaction provided by zinc coatings. A similar trend was observed for both the minimum and maximum values, which further reinforced the consistency of these results. For the neem-coated specimens, the maximum ultimate load increased from 28.04 kN (uncoated) to 40.20 kN, with a corresponding increase in the maximum bond strength from 1.92 MPa to 2.76 MPa. Zinc-coated samples achieved even higher values, reaching a maximum ultimate load of 44.23 kN and a bond strength of 3.03 MPa, along with the lowest maximum slip-page of 3.28 mm compared to 6.11 mm in uncoated specimens. Similarly, in the minimum range, the neem-coated specimens recorded a bond strength of 2.59 MPa (vs. 1.54 MPa for uncoated), the zinc-coated specimens were further improved to 2.87 MPa, with corresponding reductions in slip-page from 5.25 mm (uncoated) to 3.45 mm (neem) and 2.86 mm (zinc). In the present study, the improvement observed in the Neem-coated specimens (2.66 MPa compared to 1.72 MPa for uncoated steel) suggests that the primary contribution to bond improvement arises from the phytochemical components of Neem, which form a thin, adsorbed, and micro-textured protective layer that maintains adequate frictional and chemical interaction with the surrounding concrete, while the binder mainly serves as a carrier for uniform coating deposition rather than as a strength-enhancing agent. Fig. 5 shows the Standard deviations along with the error bars of the measured corrosion parameters.

Overall, the results demonstrate that both neem and zinc coatings significantly enhanced the bond strength between the reinforcement and surrounding matrix, primarily by reducing slippage and increasing load-bearing capacity. While zinc coating provided the greatest improvement across all parameters, neem coating displayed nearly equivalent performance, with bond strength values only marginally lower than those of zinc. This suggests that neem-based bio-coatings can serve as effective and sustainable alternatives to conventional metallic coatings, offering comparable bond-strength enhancement and improved structural performance.

The failure pattern observed during the pull-out test further revealed the enhanced performance of the organic inhibitor coatings in achieving better bond strength values. The crack patterns observed were of two types: longitudinal cracks and radial splitting cracks, as shown in Fig. 6. The extent of the crack width indicates the performance of the surface-applied corrosion inhibitor coatings in mitigating corrosion.

Fig. 6 clearly shows that the uncoated specimen had a higher crack width, indicating proper debonding of the rebar from concrete, whereas the coated rebar showed very minute radial cracks, indicating a better bond between concrete and steel, affirming the performance of surface-applied corrosion inhibitors in mitigating corrosion. This section highlights the integration of advanced image processing techniques with half-cell potential experiments for a comprehensive analysis of corrosion in reinforced steel bars. This methodology combines precise experimental data with computational algorithms to enhance the accuracy and reliability of corrosion rate and pattern assessments.

4.3. Surface Morphology using Scanning Electron Microscopy

SEM analysis revealed marked differences in the surface morphologies of the uncoated and neem-coated steel specimens (Fig. 7). The uncoated surface exhibited a highly irregular and porous morphology, with extensive cracks and pits covering approximately 30–40% of its surface area. The associated corrosion products were voluminous, flaky, and

Fig. 6: a) Pull-out test, b) Uncoated samples, c) Coated samples.

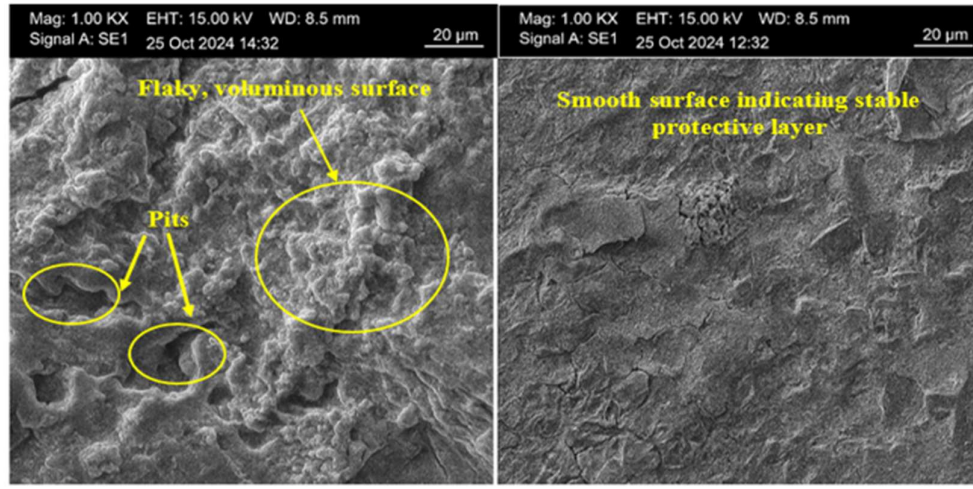

Fig. 7: SEM micrographs showing the surface morphology of (a) uncoated corroded steel and (b) Neem-coated steel after exposure to chloride-induced corrosion, captured at 1.00 kX magnification with a 20 µm scale bar.

loosely bound, indicating unstable growth and progressive material deterioration. In contrast, neem-coated steel displayed a relatively smoother and more compact surface, characterized by only minor localized defects. The corrosion products formed on this surface were minimal and firmly adherent, suggesting the development of a more stable and protective layer that effectively mitigated corrosion.

5. INTERPRETATION OF RESULTS

The experimental results show that Azadirachta indica (Neem) powder is an effective corrosion inhibitor for steel reinforcement in chloride-rich environments, performing nearly as well as a conventional zinc coating. Half-cell potential measurements decreased by 47.5% for Neem and 45.0% for zinc, indicating that both coatings successfully reduced the electrochemical activity responsible for steel depassivation. These reductions persisted for 365 days, demonstrating Neem's long-term protective capability under aggressive conditions and confirming its effectiveness at the reinforcement level. Weight and diameter loss measurements further supported these findings, as Neem-coated rebars showed a 25.3% reduction in mass loss and a 5.8% decrease in diameter loss compared to uncoated bars, indicating that the coating acts as a physical barrier that limits chloride ingress and slows corrosion. SEM analysis revealed a compact surface morphology with minimal corrosion products on the neem-coated bars, whereas the uncoated samples exhibited extensive pitting and flaky rust covering 30–40% of the surface. Bond strength tests indicated that Neem coatings improved the steel–concrete interface by 54.6% relative to uncoated bars, approaching the performance of zinc. This demonstrates the dual benefit of Neem in reducing corrosion while maintaining critical bond strength, which is essential for structural safety.

From a sustainability perspective, life cycle assessment showed that neem coatings reduce the carbon footprint by up to 43% compared to zinc and lower the cost per meter of reinforcement coating by 39.6%.

Overall, Neem-based organic coatings provide a sustainable and economically viable alternative to metallic inhibitors. Neem offers comparable corrosion protection, preserves structural integrity, and supports environmentally friendly construction, positioning it as a promising material for green, durable, and cost-effective infrastructure protection.

6. LIFE CYCLE ASSESSMENT AND ENVIRONMENTAL IMPACT

The environmental impact of corrosion protection for reinforced concrete highlights the link between structural durability and sustainability. Life cycle assessments have shown that neem-based coatings offer significant ecological advantages over traditional chromate and zinc systems, reducing the carbon footprint by up to 43% while providing equal or better corrosion protection (Banumathi et al. 2024). Conventional coatings, particularly those containing hexavalent chromium, pose environmental hazards through toxic waste generation and carcinogenic risks, necessitating careful disposal (Abuelela et al. 2023). Neem (Azadirachta indica) extract demonstrates high corrosion inhibition, achieving up to 97% efficiency for carbon steel in chloride environments, improving from 75% over 72 h (Okewale & Omoruwuo 2018). Neem inhibitors are plant-derived, biodegradable, and non-toxic. They are sourced from

renewable biomass, reducing environmental impact and sequestering carbon during their growth. ISO 14040-based life cycle assessments indicate that neem coatings emit as little as 1.5–2.6 kg CO_2 eq.kg^{-1}, compared to higher emissions from conventional systems (Borgaonkar & McNamara 2024). They also reduce ozone depletion, fossil fuel consumption, and heavy metal contamination associated with chromate-based coatings.

Life Cycle Assessment (LCA) was conducted in accordance with ISO 14040/14044 standards to compare the environmental impacts of neem-based and zinc-based coatings. The functional unit (FU) selected for this study was defined as 1 m² of coated reinforcement steel, as this unit allows a performance-based comparison that is independent of material density or coating thickness. The system boundaries followed a 'cradle-to-gate' approach, including raw material extraction, processing, manufacturing of coating components, and transportation to the construction site. End-of-life impacts and maintenance cycles were excluded because of insufficient standardized datasets for organic coating degradation. Inventory data for neem powder production were obtained from local supplier datasets and supplemented with regional agricultural emission factors, while zinc-related emission values were sourced from secondary datasets reported in ecoinvent v3.9 and published LCI databases. Linseed oil emissions were derived from standard vegetable oil processing data sets. All emissions were converted to global warming potential (GWP) expressed as kg CO_2-eq using the IPCC 2021 characterization factors. Based on these inputs, the estimated carbon footprint of the Neem coating was 1.14 kg CO_2-eq per m² of coated steel, compared to 2.00 kg CO_2-eq per m² for the zinc coating, corresponding to an approximate 43% reduction in embodied carbon. These values reflect only the material impacts and do not account for potential differences in service life extension. The cost and carbon savings were normalized to the same functional unit (1 m² of coated steel), ensuring a performance-equivalent comparison. This normalization avoids misinterpretations that could arise from weight-based comparisons alone, especially given the differing densities and application rates of organic and metallic coatings. The study demonstrates that neem coatings can reduce corrosion-induced weight loss by 72% and improve half-cell potential values by 75% compared to uncoated bars while maintaining eco-safety. These properties make neem a sustainable alternative that lowers long-term environmental and economic costs, extends the structural service life, and minimizes chemical waste. The use of neem supports a circular economy by valorizing natural resources, enhancing structural durability, and contributing to global sustainability and pollution reduction goals, as shown in Fig. 8.

7. COST-BENEFIT ANALYSIS

The cost analysis of the coating systems revealed significant variations in material expenditure depending on the inhibitor type and the coating thickness. The details of the various materials used in this study, as per the current market rate, are provided in Table 5.

Furthermore, the total cost required to coat one bar with a single coat of the inhibitors comprises the cost of the inhibitor and the cost of the oil. The details of the total cost are provided in table.

Table 5: Cost of inhibitors.

Material	Approximate Price [Maximum]	Source
Neem Powder	Rs. 400.kg^{-1}	Indiamart (2025)
Zinc Powder	Rs. 900.kg^{-1}	Indiamart (2025)

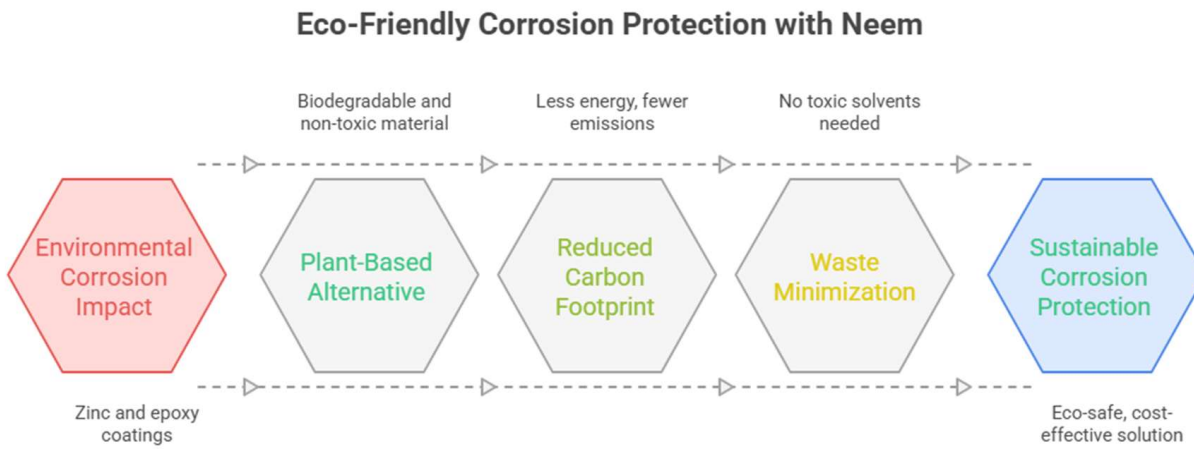

Fig. 8: Benefits of neem inhibitor coatings.

Table 6: Cost per coat of the inhibitors.

Coating Type	Thickness	Inhibitor Req. [g]	Oil Req. [mL]	Cost of Inhibitor [₹]	Cost of Oil [₹]	Total Cost [₹]	Cost per Coat [₹]	Cost per coat.m^{-1} [₹]
Neem	1 coat	18	26	7.2	6.5	13.7	6.85	22.83
Zinc	1 coat	18	26	16.2	6.5	22.7	11.35	37.83

The cost analysis presented in Tables 5 and 6 is based on market prices obtained from suppliers in India, with all rates verified between January and July 2025 to ensure their current relevance. The material costs for neem, zinc, and linseed oil were obtained from regional wholesale markets and manufacturer quotations, reflecting typical procurement scenarios in Indian construction practice. The calculated cost reduction of 39.6% for the neem-based coating compared to zinc is representative of the prevailing local market conditions. As evident from the cost analysis of the coatings, the per coat cost obtained in the present study for neem-coated specimens was Rs 6.85, and for zinc-coated specimens, it was Rs 11.35. Furthermore, if the cost is calculated for per meter length of the reinforcement bar, there is almost a 39.6% reduction in the coating cost. This proves that organic inhibitor coatings are an economically viable alternative to harmful chemical-based coatings.

8. CONCLUSION AND FUTURE SCOPE

This study evaluated the performance of Azadirachta indica (Neem) powder as a sustainable corrosion inhibitor coating for reinforcing steel in chloride-induced environments and benchmarked its effectiveness against zinc coatings. The findings confirmed that neem-based coatings significantly enhanced corrosion resistance and structural performance while offering economic and environmental advantages. Quantitatively, the neem-coated specimens achieved a 47.5% reduction in half-cell potential, a 25.3% reduction in weight loss, and a 5.8% reduction in diameter loss, closely matching the performance of zinc coatings. The bond strength improved from 1.72 MPa in uncoated specimens to 2.66 MPa with Neem coatings, representing a 54.6% improvement and approaching the performance of zinc-coated bars (2.95 MPa). SEM analysis further validated the protective action of neem through compact surface morphology and minimal corrosion products. Beyond technical performance, Neem coatings demonstrated up to a 43% reduction in carbon footprint and a 39.6% lower cost per meter of reinforcement protection, underlining their potential as an eco-friendly and economically viable alternative to conventional metallic inhibitors. This study had certain limitations that should be acknowledged. The experiments were conducted using a single coating thickness and a relatively small sample size, which may not fully capture the variability expected in large-scale construction applications. Additionally, all tests were performed under controlled laboratory conditions using accelerated chloride exposure, and the results may differ under natural environmental cycles involving temperature fluctuations, carbonation, and long-term wet–dry exposures. Future studies incorporating multiple coating thicknesses, larger specimen sets, and field-scale validation would help strengthen the generalizability of the findings. Future research should focus on the field-scale validation of neem coatings under varying climatic and environmental conditions, as well as the long-term performance in cracked concrete, where the ingress of chlorides is more critical. Investigations into hybrid systems combining neem with supplementary cementitious materials or nanomaterials could further optimize performance. Additionally, mechanistic studies at the molecular level, combined with machine learning-driven predictive modeling, may provide deeper insights into the durability, dosage optimization, and life cycle cost benefits of neem-based inhibitors.

Overall, this study establishes Neem as a promising bio-based technology that integrates structural durability with sustainability, supporting the transition towards greener and more resilient construction practices.

9. ACKNOWLEDGMENTS

The authors extend their acknowledgment to the Department of Civil Engineering, Sharda University, for providing access to their labs for the experimentation work.

10. REFERENCES

Abirami, R. and Sangeetha, S.P., 2022. Effect of surface modification on the characteristics of sisal fiber reinforced concrete treated with Na_2CO_3. *Nature Environment and Pollution Technology*, 21(1), pp.289-295. [DOI]

Abuelela, A.M., Kaur, J., Saxena, A., Bedair, M.A., Verma, D.K. and Berdimurodov, E., 2023. Electrochemical and DFT studies of *Terminalia bellerica* fruit extract as an eco-friendly inhibitor for the corrosion of steel. *Scientific Reports*, 13(1), p.19367. [DOI]

Al-Amiery, A., Wan Isahak, W.N.R. and Al-Azzawi, W.K., 2024. Sustainable corrosion inhibitors: a key step towards environmentally responsible corrosion control. *Ain Shams Engineering Journal*, 15(5), p.102672. [DOI]

Bajaj, D. and Khurpade, P.D., 2024. An eco-friendly Mangifera indica leaf extract corrosion inhibitor for stainless steel in an acidic medium. *Nature Environment and Pollution Technology*, 23(1), pp.139-150. [DOI]

Banumathi, R., Abuthahir, S.S.S., Sheit, H.M.K., Mohan, K.S., Mohandas,

T. and Vijaya, K., 2024. Corrosion inhibition potential of aqueous extract of trifolium repens plant leaves on carbon steel in hydrochloric acid medium (trpl). *Discover Electrochemistry*, 1(1), p.13. [DOI]

Bolzoni, F., Brenna, A. and Ormellese, M., 2022. Recent advances in the use of inhibitors to prevent chloride-induced corrosion in reinforced concrete. *Cement and Concrete Research*, 154(1), p.106719. [DOI]

Borgaonkar, A. and McNamara, G., 2024. Environmental impact assessment of anti-corrosion coating life cycle processes for marine applications. *Sustainability*, 16(13), p.5627. [DOI]

Cao, N.L., Shevtsov, D.S., Nguyen, V.C., Nguyen, D.A., Le, H.Q., Tran, V.T., Nguyen, V.T., Nguyen, N.H., Zartsyn, I.D. and Briyalovskaya, E.S., 2025. Migrating corrosion inhibitors for steel reinforcement in concrete under chloride activation: a review. *International Journal of Corrosion and Scale Inhibition*, 14(2), pp.469-490. [DOI]

Casanova, L., Ceriani, F., Messinese, E., Paterlini, L., Beretta, S., Bolzoni, F.M., Brenna, A., Diamanti, M.V., Ormellese, M. and Pedeferri, M.P., 2023. Recent advances in the use of green corrosion inhibitors to prevent chloride-induced corrosion in reinforced concrete. *Materials*, 16(23), p.7462. [DOI]

Chen, Y., Chen, M., Chen, R. and Kang, X., 2023. Deterioration mechanism of chloride attack on reinforced concrete under stray current and high hydraulic pressure coexistence environment. *Materials and Structures*, 56(9), p.160. [DOI]

De Schutter, G. and Luo, L., 2004. Effect of corrosion-inhibiting admixtures on concrete properties. *Construction and Building Materials*, 18(7), pp.483-489. [DOI]

Ega, I.J., Job, O.F., Anowai, I.S. and Dakas, A.I.I., 2024. Durability characteristics of corn-cob ash (CCA) blended cement concrete. *Journal of Materials and Manufacturing Technology*, 1(1), pp.1-8. [DOI]

Ghanaati, B., Irannejad, A. and Raveri, F.B., 2022. Production and investigating the effect of Echium amoenum Fisch-8me (part of stem and leaf, wastes) extract as a green and cheap corrosion inhibitor on St37 steel in a 3.5 wt% NaCl corrosive medium. *Journal of Corrosion Science and Technology*, 1(1), pp.1-12. [DOI]

Hao, H., Bi, K., Chen, W., Pham, T.M. and Li, J., 2023. Towards next-generation design of sustainable, durable, multi-hazard resistant, resilient, and smart civil engineering structures. *Engineering Structures*, 277(1), pp.115477. [DOI]

Jiang, C., Wei, G.-F., Lei, R., Deng, S., Li, X. and Shao, D., 2025a. Functional development of extracts from the invasive plant water hyacinth for steel corrosion protection. *Npj Materials Degradation*, 9(1), p.33. [DOI]

Jiang, M., Liu, X., Xu, Y., Li, S., Liu, X., Niu, X., Lu, L., Sun, X., Xie, Z., Wang, Z. and Cui, S., 2025b. Corrosion inhibition effect and mechanism of eco-friendly corrosion inhibitors on mild steel in simulated concrete pore solution: experimental and theoretical studies. *ACS Sustainable Chemistry & Engineering*, 13(6), pp.2411-2428. [DOI]

Goni, L.K.M.O. and Mazumder, M.A.J., 2019. Green corrosion inhibitors. In: Corrosion Inhibitors. IntechOpen. [DOI]

Kamarska, K.V., 2024. Investigation of rosemary oil as an environmentally friendly corrosion inhibitor of aluminum alloy. *Nature Environment and Pollution Technology*, 23(3), pp.1723-1727. [DOI]

Krishnanjana, K. and Ganesh, G.M., 2025. Green corrosion inhibition of *Punica granatum* peel powder on tmt in salt medium: outlooks from experiments and artificial neural networks. *Green Chemistry Letters and Reviews*, 18(1), pp.1-12. [DOI]

Kumar, N., Mohd Noor, I.S., Zu Azhan Yahya, M. and Prakash, S., 2025. Botanical corrosion inhibitors in reinforced concrete: material sustainability assessment and analysis - A review. *Materials Protection*, 66(1), pp.40-55. [DOI]

Kumar, N. and Saharan, S., 2022. Use of *Lawsonia inermis* and sodium nitrite as surface applied corrosion inhibitors. *International Journal of Sustainable Construction Engineering and Technology*, 13(1), pp.1-10. [DOI]

Li, Z., Long, Z., Lei, S., Liu, X., Yang, L., Zhang, W. and Zhang, T., 2023. Evaluating the corrosion resistance of marine steels under different exposure environments via machine learning. *Physica Scripta*, 98(1), p.015402. [DOI]

Liu, J., Hang, M., Jiang, M. and Song, H., 2025. Rust inhibition mechanism of reinforced concrete by alcohol-amine corrosion inhibitor under the coupling of composite salt erosion, freeze-thaw cycle and dry-wet cycle. *Case Studies in Construction Materials*, 22(1), p.e04466. [DOI]

Liu, Q., Yuan, M., Zhang, J. and Qiang, S., 2024. Research on the corrosion inhibition effect of *Xanthium sibiricum* on reinforced steel and the prediction of reinforced concrete performance under a stray current and chloride environment. *Applied Sciences*, 14(16), p.6986. [DOI]

Liu, Y. and Shi, J., 2024. Recent progress and challenges of using smart corrosion inhibitors in reinforced concrete structures. *Construction and Building Materials*, 411(1), p.134595. [DOI]

McCafferty, E., 2010. Introduction to Corrosion Science. Springer, p.575. [DOI]

Montes-García, P., Jiménez-Quero, V. and López-Calvo, H., 2015. Assessment of high-performance concrete containing fly ash and calcium nitrite-based corrosion inhibitor as a means to prevent the corrosion of reinforcing steel. *Journal of Physics: Conference Series*, 582(1), p.012028. [DOI]

Nóvoa, X.R. and Pérez, C., 2023. The use of smart coatings for metal corrosion control. *Current Opinion in Electrochemistry*, 40(1), p.101324. [DOI]

Okeniyi, J., Loto, C. and Popoola, A., 2016. Effects of *Phyllanthus muellerianus* leaf extract on steel-reinforcement corrosion in 3.5% NaCl-immersed concrete. *Metals*, 6(11), p.255. [DOI]

Okeniyi, J.O., Popoola, A.P.I. and Okeniyi, E.T., 2018. Cymbopogon citratus and nano2 behaviors in 3.5% NaCl-immersed steel-reinforced concrete: Implications for eco-friendly corrosion inhibitor applications for steel in concrete. *International Journal of Corrosion*, 2018(1), pp.1-11. [DOI]

Okewale, A. and Omoruwuo, F., 2018. Neem leaf extract as a corrosion inhibitor on mild steel in acidic solution. *International Journal of Engineering Research in Africa*, 35(1), pp.208-220. [DOI]

Ovari, T.-R., Brânzanic, A.M.V., Katona, G., Szabó, G.S. and Muresan, L.M., 2025. New eco-friendly corrosion inhibitor for zinc based on expired Detralex drug. Adsorption, electrochemical and computational studies. *Materials Today Communications*, 46(1), p.112739. [DOI]

Sharma, N., Sharma, S., Sharma, S.K., Mahajan, R.L. and Mehta, R., 2022. Evaluation of corrosion inhibition capability of graphene modified epoxy coatings on reinforcing bars in concrete. *Construction and Building Materials*, 322(1), p.126495. [DOI]

Sharmila, S.M. and Vasanthi, P., 2024. Performance evaluation of corrosion protective coatings on marine concrete piles: an experimental study utilizing artificial neural network and statistical analysis. *Asian Journal of Civil Engineering*, 25(4), pp.3059-3080. [DOI]

Shehnazdeep and Pradhan, B., 2022. A study on the effectiveness of inorganic and organic corrosion inhibitors on rebar corrosion in concrete: a review. *Materials Today: Proceedings*, 65(1), pp.1360-1366. [DOI]

Singh, R., Arora, H.C., Bahrami, A., Kumar, A., Kapoor, N.R., Kumar, K. and Rai, H.S., 2022. Enhancing the sustainability of corroded RC structures: estimating steel-to-concrete bond strength with ANN and SVM algorithms. *Materials*, 15(23), p.8295. [DOI]

Söylev, T.A. and Richardson, M.G., 2008. Corrosion inhibitors for steel in concrete: state-of-the-art report. *Construction and Building Materials*, 22(4), pp.609-622. [DOI]

Suhas, V.S., Shanmugapriya, T., Borg, R.P., Akash, K. and Sunil, A., 2025. Enhanced corrosion inhibition of mild steel in concrete pore solution using modified MgO-chitosan epoxy nanocomposite coatings. *Materials Letters*, 398(1), p.138916. [DOI]

Tarabin, M., Maalej, M., Altoubat, S. and Talha Junaid, M., 2023. Review of the bond behavior between reinforcing steel and engineered cementitious composites. *Structures*, 55(1), pp.2143-2156. [DOI]

Umamathi, T., Prathipa, V., Roslin, A., Jewelcy, A.L., Jeevithe Clara, M.V., Anitha, N., Nasrin Sahana, M.I., Susai, R. and Krishnaveni, A., 2024. Influence of sodium chloride on corrosion resistance of ever silver vessels in the presence of curd rice. *Materials Protection*, 65(4), pp.765-777. [DOI]

Verma, C., Kumar, A. and Thakur, A., 2024. Phytochemistry in Corrosion Science: Plant Extracts and Phytochemicals as Corrosion Inhibitors. CRC Press, p.532. [DOI]

Zhao, A., Sun, H., Chen, L., Huang, Y., Lu, X., Mu, B., Gao, H., Wang, S. and Singh, A., 2019. Electrochemical studies of bitter gourd (Momordica charantia) fruits as eco-friendly corrosion inhibitor for mild steel in 1 M HCl solution. *International Journal of Electrochemical Science*, 14(7), pp.6814-6825. [DOI]